EFFECT OF ALBEDO ON THE MOTION OF THE INFINITESIMAL BODY IN CIRCULAR RESTRICTED THREE BODY PROBLEM WITH VARIABLE MASSES

Abdullah A. Ansari
Department of Mathematics
College of Science in Al-Zulfi
Majmaah University
Kingdom of Saudi Arabia
a.ansari@mu.edu.sa

Abstract. This paper presents the investigation of the effect of Albedo on the motion of the infinitesimal body in the circular restricted three body problem with the variation of all masses (primaries as well as infinitesimal body) with time. The radiation pressures fall on the surfaces of the planets, some of radiations are absorbed by them but some radiations are reflected back into the space. These radiations from the planets to the space are known as Albedo (i.e. Albedo = (radiation reflected back into the space)/(incident radiation)).

The equations of motion have been evaluated by using Meshcherskii transformation and found the expression for the variation of the Jacobi integral constant. We have drawn the locations of the equilibrium points, the periodic orbits, Poincaré surface of sections and basins of attraction for four cases (a. Classical Case, b. Variation of mass, c. Solar radiation pressure effect, d. Albedo effect) and also the surfaces of the motion of the infinitesimal body have been drawn with the effect of Albedo only.

Finally, we have examined the stability of the equilibrium points under the effect of Albedo and found that all the equilibrium points are unstable.

Keywords: CR3BP, Variable masses, Albedo, Radiation pressure, Periodic orbits, Poincaré surface of sections, Basins of attraction.

1. Introduction

In our solar system, there are many stars which are source of radiations, one of them is sun. Due to it, the radiation spreads on the planets and after absorbtion of the radiation by the planets, some radiations reflected back into the space. This reflected radiation is known as Albedo (i.e. Albedo = (radiation reflected back into the space)/(incident radiation)).

The most common problem in the celestial mechanics is the restricted three body problem in which two finite bodies called primaries move around their center of mass in the circular or elliptic orbits under the influence of their mutual gravitational attraction and a third body of the infinitesimal mass is moving in the plane of the primaries, which is influenced by them but not influencing them.

Many scientist studied this model by taking different perturbations as different shapes of the primaries, the solar radiation pressure, the resonance, the variation of masses, the coriolis and centrifugal forces, the Yarkovsky effect, the Poynting-Robertson drags, Albedo effect etc.

The two body problem with variable mass has been discussed by Jeans [19]. Meshcherskii [23] worked on the mechanics of bodies of variable mass. Chernikov [14] studied the stability of equilibrium points by Lyapunov's methods in the restricted three body problem with the effects of solar radiation pressure but the effect of albedo is not considered by him. Perezhogin [28] studied the stability of the sixth and seventh libration points in the photogravitational circular restricted three body problem. Bhatnagar et al. [11, 12] investigated about the equilibrium points in the photogravitational restricted three body problem. They examined the stability of the equilibrium points and observed that the equilibrium points are stable in the linear sense and unstable around the triangular points. Schuerman [31] studied the restricted three body problem including the force of radiation pressure and the Poynting-Robertson effect and found that the triangular equilibrium points are depending on both the solar radiation pressure and the Poynting-Robertson drag. Anselmo et al. [7] studied the effect of Albedo on the orbit of the LAGEOS satellite and proposed that the periodic perturbations is due to Albedo. Mignard [24] studied the restricted three-body problem with the solar radiation pressure. And observed that triangular equilibrium points are no longer exist. Kunitsyn et al. [21] proved the existence of the three-parametric family of the collinear libration points in the photo-gravitational three-body problem. They determined the number and locations of these points and also they examined the stability and found that the points are stable for some domain of parameter space.

Simmons et al.[34] investigated the restricted 3-body problem with radiation pressure and observed that nine equilibrium points exist, five in the plane of motion and four in the out of plane. Sharma [32, 33] investigated the stationary solutions of the planar restricted three-body problem when the more massive primary is a source of radiation and smaller primary is an oblate spheroid with its equatorial plane coincident with the plane of motion. Appel [8] developed a numerical model for altitude estimation from magnetometer and earth-albedo-corrected coarse sun sensor measurement. AbdulRaheem et al. [1] investigated the stability of equilibrium points under the influence of the Coriolis and centrifugal forces together with the effects of oblateness and radiation pressure of the primaries. It is observed that the collinear points are unstable and the triangular points are conditionally stable depending on the radiation factor and oblateness. It is also observed that the Coriolis force has a stabilizing tendency, while the centrifugal force, radiation and oblateness of the primaries have destabilizing effects. Rocco [30] investigated the evaluation of the terestial albedo applies to some scientific missions and calculated the irradiance at the satellite with the radiant flux from each cell. Singh et al. [35, 36, 37, 38, 39] studied about the effect of small perturbations in the Coriolis and centrifugal forces on

the locations and stability of the equilibrium points in the restricted three body problem and Robe's restricted three body problem with the variable mass. Ershkov [16] extend the photo-gravitational three-body problem with additional effect of Yarkovsky. Zhang et al.[41] studied about the triangular libration points in photo-gravitational restricted three body problem with variable mass. They have used the space time inverse transformation of Meshcherskii for the linear stability of the triangular points and observed that the motion around the triangular points are unstable with decreasing mass. Abouelmagd et al. [2, 3] studied the effect of oblateness in the perturbed restricted three body problem and also with variable mass. And they found an appropriate approximation for the locations of out-of-plane equilibrium points in the special case of a non-isotropic variation of the mass. They determined the elements of periodic orbits and periodicity around these points under the effects of the perturbations.

Ansari [4] investigated the stability of the equilibrium points in the photo-gravitational circular restricted four body problem with the effect of variable masses, coriolis and centrifugal forces. He used the Jeans law and Meshcherskii law in the space time transformations. It is observed that there exists eight equilibrium points in which three points are asymptotically stable and five points are unstable. Mittal et al. [25] investigated the stability of the Lagrangian solutions for the restricted four-body problem with variable mass. They found at most eight libration points in which two are collinear and rests are non-collinear and observed that all the libration points are unstable. Idrisi [17, 18] investigated the effects of albedo on the libration points and its stability in the restricted three body problem when less massive primary is an ellipsoid. He found five libration points in which three unstable collinear libration points and two stable non-collinear libration points. On the other hand, many scientists have studied about the basin of attraction in both R3BP and R4BP cases. Douskos [15], Assis et al. [10], Kumari et al. [20], Asique et al. [9], Matthies [22], Paricio [27], Ansari [5, 6], Zotos [42, 43, 44, 45].

We have studied the effect of Albedo on the motion of the infinitesimal body in the circular restricted three body problem in which the masses of the primaries as well as the mass of the infinitesimal body vary with time. We have studied our problem in various sections. In the equations of motion section, we have evaluated the equations of motion of the infinitesimal variable mass under the effects of the Albedo and also determined the expression for the variation of Jacobi Integral constant. In the Numerical Analysis section, we have plotted the equilibrium points, the periodic orbits, Poincaré surface of sections and basins of attraction in four cases and also the surfaces of the motion of the infinitesimal body have been drawn under the effect of Albedo only. In the stability section, we have examined the stability of the equilibrium points under the effect of Albedo only. And finally, we have concluded the problem.

Our problem has many applications in scientific research, not only in the fields of celestial mechanics but also in physics and quantum mechanics.

2. Equations of motion

Let there be three variable masses $m_1(t)$, $m_2(t)$ and $m(t)$. The two primary bodies $m_1(t)$ and $m_2(t)$ are moving in the circular orbits around their center of mass O which is considered as origin. The third infinitesimal body $m(t)$ is moving in the plane of motion of $m_1(t)$ and $m_2(t)$ under their gravitational forces F_1 and F_2 respectively but not influencing them. The body $m_1(t)$ is a source of radiation pressure such that $m_1(t) > m_2(t)$. F_p is the solar radiation pressure on $m(t)$ due to $m_1(t)$ and F_a is the Albedo force (solar radiation reflected by $m_2(t)$ in space on $m(t)$). Let the inertial and rotating frames be (XYZ) and (xyz) respectively with the same origin. We also assume that the coordinates of $m_1(t)$, $m_2(t)$ and $m(t)$ in the inertial frame are $(X_1, Y_1, Z_1), (X_2, Y_2, Z_2)$ and (X, Y, Z), while in the rotating frame they are $(x_1, 0, 0), (x_2, 0, 0)$ and (x, y, z) respectively (Fig. 1).

The forces acting on $m(t)$ due to $m_1(t)$ and $m_2(t)$ are $F_1(1-\varepsilon_1)$ and $F_2(1-\varepsilon_2)$ respectively, where $\varepsilon_1 = F_p/F_1 << 1$ and $\varepsilon_2 = F_a/F_2 << 1$. And also ε_1 and ε_2 can be expressed as $\varepsilon_1 = \frac{L_1}{2\pi G m_1(t) c\sigma}$, $\varepsilon_2 = \frac{L_2}{2\pi G m_2(t) c\sigma}$, where L_1 and L_2 are the luminosity of $m_1(t)$ and $m_2(t)$ respectively, G is the gravitational constant, c is the speed of light and σ is the mass per unit area of the infinitesimal mass $m(t)$. $\frac{\varepsilon_2}{\varepsilon_1} = \frac{m_1(t)L_2}{m_2(t)L_1} = \frac{m_1(t)}{m_2(t)}k_0$, $\frac{L_2}{L_1} = k_0$ (constant), $0 \le \varepsilon_1 < 1, 0 \le \varepsilon_2 < \varepsilon_1$ and $0 \le k_0 < 1$.

The equations of motion of the infinitesimal variable mass with the solar radiation pressure and albedo effect in the inertial frame of reference under the assumptions that the masses that fall on (or ejected from) the bodies have zero momentum, are

$$(1)\qquad \begin{cases} \frac{\dot{m}(t)}{m(t)}\dot{X}+\ddot{X}=-\frac{Gm_1(t)(X-X_1)(1-\varepsilon_1)}{r_1^3}-\frac{Gm_2(t)(X-X_2)(1-\varepsilon_2)}{r_2^3}, \\ \frac{\dot{m}(t)}{m(t)}\dot{Y}+\ddot{Y} = -\frac{Gm_1(t)Y(1-\varepsilon_1)}{r_1^3} - \frac{Gm_2(t)Y(1-\varepsilon_2)}{r_2^3}, \\ \frac{\dot{m}(t)}{m(t)}\dot{Z} + \ddot{Z} = -\frac{Gm_1(t)Z(1-\varepsilon_1)}{r_1^3} - \frac{Gm_2(t)Z(1-\varepsilon_2)}{r_2^3}. \end{cases}$$

where, $r_i^2 = (X-X_i)^2+Y^2+Z^2, (i = 1, 2)$, are the distances from the primaries to the infinitesimal body in the inertial coordinate frame respectively.
The relation between the inertial and the rotating coordinates which has angular velocity $\omega(t)$, is governed by

$$(2)\qquad \begin{cases} X = x\ cos(\omega(t)t) - y\ sin(\omega(t)t), \\ Y = x\ sin(\omega(t)t) + y\ cos(\omega(t)t), \\ Z = z. \end{cases}$$

Substituting system (2) in system (1), the equations of motion of the infinitesimal variable mass in rotating coordinate system when the variation of masses

is non-isotropic, become

$$
(3)\qquad \begin{cases} \dfrac{\dot{m}(t)}{m(t)}(\dot{x}-\omega(t)\ y)+(\ddot{x}-\dot{\omega(t)}\ y-2\omega(t)\ \dot{y}-\omega^2(t)x) \\ =-\dfrac{\mu_1(t)(x-x_1)(1-\varepsilon_1)}{r_1^3}-\dfrac{\mu_2(t)(x-x_2)(1-\varepsilon_2)}{r_2^3}, \\ \dfrac{\dot{m}(t)}{m(t)}(\dot{y}+\omega(t)\ x)+(\ddot{y}+\dot{\omega(t)}\ x+2\omega(t)\ \dot{x}-\omega^2(t)\ y) \\ =-\dfrac{\mu_1(t)y(1-\varepsilon_1)}{r_1^3}-\dfrac{\mu_2(t)y(1-\varepsilon_2)}{r_2^3}, \\ \dfrac{\dot{m}(t)}{m(t)}\dot{z}+\ddot{z}=-\dfrac{\mu_1(t)z(1-\varepsilon_1)}{r_1^3}-\dfrac{\mu_2(t)z(1-\varepsilon_2)}{r_2^3}. \end{cases}
$$

where, $r_i^2=(x-x_i)^2+y^2+z^2,(i=1,2)$, are the distances from the primaries to the infinitesimal body in the rotating coordinate system respectively, $\mu_i(t)=G\ m_i(t),(i=1,2)$.

Using Meshcherskii transformation

$$
\begin{aligned}
&x=\xi R(t),\ y=\eta R(t),\ z=\zeta R(t),\frac{dt}{d\tau}=R^2(t),r_i=\rho_i R(t),\\
&\omega(t)=\frac{\omega_0}{R^2(t)},x_i=\xi_i R(t),\\
&\mu(t)=\mu_1(t)+\mu_2(t)=\frac{\mu_0}{R(t)},\mu_i(t)=\frac{\mu_{i0}}{R(t)},\\
&m(t)=\frac{m_0}{R(t)},R(t)=\sqrt{a\ t^2+2b\ t+c},
\end{aligned}
$$

where a,b,c,μ_0,μ_{i0},m_0 are constants for $i=1,2$.

$$
(4)\qquad \begin{cases} \dot{x}=\dfrac{\xi'+(a\ t+b)\xi}{R(t)},\ddot{x}=\dfrac{\xi''+(a\ c-b^2)\xi}{R^3(t)} \\ \dot{y}=\dfrac{\eta'+(a\ t+b)\eta}{R(t)},\ddot{y}=\dfrac{\eta''+(a\ c-b^2)\eta}{R^3(t)} \\ \dot{z}=\dfrac{\zeta'+(a\ t+b)\zeta}{R(t)},\ddot{z}=\dfrac{\zeta''+(a\ c-b^2)\zeta}{R^3(t)}. \end{cases}
$$

The system (3) becomes

$$
(5)\qquad \begin{cases} \xi''-2\omega_0\eta'-(at+b)\xi'=\dfrac{\partial W}{\partial \xi}, \\ \eta''+2\omega_0\xi'-(at+b)\eta'=\dfrac{\partial W}{\partial \eta}, \\ \zeta''-(at+b)\zeta'=\dfrac{\partial W}{\partial \zeta}. \end{cases}
$$

where,

$$W = \frac{1}{2}((at+b)^2 + \omega_0^2 - (ac-b^2))(\xi^2+\eta^2) + \frac{1}{2}((at+b)^2 - (ac-b^2))\zeta^2$$
$$- (a\,t+b)\xi\eta + \frac{\mu_{10}(1-\varepsilon_1)}{\rho_1} + \frac{\mu_{20}(1-\varepsilon_2)}{\rho_2},$$
$$\rho_i^2 = (\xi-\xi_i)^2 + \eta^2 + \zeta^2, \xi_1 = \frac{\mu_{20}}{\mu_0}R_{12}, \xi_2 = \frac{-\mu_{10}}{\mu_0}R_{12}$$

Prime ($'$) is the differentiation w.r.to τ. R_{12} is the distance between the primaries. Taking unit of mass, distance and time at initial time t_0 such that

$$\mu_0 = 1,\ G = 1,\ R_{12} = 1,\ \omega_0 = 1,\ at_0 + b = \alpha_1 \text{ (constant)}.$$

Introducing the new mass parameter as

$$\frac{\mu_{10}}{\mu_0} = 1 - \upsilon,\ \frac{\mu_{20}}{\mu_0} = \upsilon, 0 < \upsilon \leq \frac{1}{2}$$

and

$$\varepsilon_2 = \frac{\varepsilon_1(1-\upsilon)}{\upsilon}k_0,$$

where υ is the ratio of the mass of the primaries to the total mass of the primaries.

Finally, the system (5) becomes

$$\begin{cases} \xi'' - 2\eta' - \alpha_1\xi' = \dfrac{\partial\psi}{\partial\xi}, \\ \eta'' + 2\xi' - \alpha_1\eta' = \dfrac{\partial\psi}{\partial\eta}, \\ \zeta'' - \alpha_1\zeta' = \dfrac{\partial\psi}{\partial\zeta}. \end{cases} \tag{6}$$

where,

$$\psi = \frac{1}{2}(\alpha_1^2 + k)(\xi^2+\eta^2+\zeta^2) - \frac{1}{2}\zeta^2 - \alpha_1\xi\eta + \frac{(1-\upsilon)(1-\varepsilon_1)}{\rho_1} + \frac{\upsilon(1-\varepsilon_2)}{\rho_2},$$
$$\rho_i^2 = (\xi-\xi_i)^2 + \eta^2 + \zeta^2, ac - b^2 = 1 - k \text{ and } \xi_1 = \upsilon, \xi_2 = \upsilon - 1.$$

If there are constant masses then there is a constant motion (i.e Moulton [26]), the Jacobi constant defined as

$$C = 2\psi - 2((\xi')^2 + (\eta')^2 + (\zeta')^2), \tag{7}$$

Multiplying in the first equation of (6) by ξ', in the second equation of (6) by η' and in the third equation of (6) by ζ' and add and using equation (7), we get the variation of the Jacobi constant as

$$\frac{dC}{d\tau} = -2\alpha_1((\xi')^2 + (\eta')^2 + (\zeta')^2), \tag{8}$$

Where C is the Jacobi Integral Constant.

3. Numerical analysis

In this section, we have plotted numerically the locations of the equilibrium points, the periodic orbits, the Poincaré surfaces of section and the basins of attraction by using Mathematica software for four different cases:

a. Classical case (i.e.$k = 1, \alpha_1 = 0, \varepsilon_1 = 0, k_0 = 0$),
b. Variation of masses (i.e. $k = 0.4, \alpha_1 = 0.2, \varepsilon_1 = 0, k_0 = 0$),
c. Solar radiation pressure (i.e. $k = 0.4, \alpha_1 = 0.2, \varepsilon_1 = 0.5, k_0 = 0$),
d. Albedo effect (i.e. $k = 0.4, \alpha_1 = 0.2, \varepsilon_1 = 0.5, k_0 = 0.015$).

And also the surfaces of the infinitesimal body have been drawn under the effect of Albedo only. In all the graphical work, the value of υ is 0.019.

3.1 Locations of Equilibrium points during in-plane and out of plane motions

In general, the locations of equilibrium points are obtained by solving $\psi_\xi = 0$, $\psi_\eta = 0$, $\psi_\zeta = 0$, but the solutions of these equations when $(\xi \neq 0, \eta \neq 0, \zeta = 0)$, represent the locations during in-plane motions (Fig. 2) and when $(\xi \neq 0, \eta = 0, \zeta \neq 0)$, $(\xi = 0, \eta \neq 0, \zeta \neq 0)$, represent the locations of the out of planes (Fig. 3, Fig. 4). Where

$$\psi_\xi = (\alpha_1^2 + k)\xi - \alpha_1\eta - \frac{(1-\upsilon)(\xi-\upsilon)(1-\varepsilon_1)}{\rho_1^3} - \frac{\upsilon(\xi-\upsilon+1)(1-\varepsilon_2)}{\rho_2^3}, \tag{9a}$$

$$\psi_\eta = (\alpha_1^2 + k)\eta - \alpha_1\xi - \frac{(1-\varepsilon_1)(1-\upsilon)\eta}{\rho_1^3} - \frac{(1-\varepsilon_2)\upsilon\eta}{\rho_2^3}, \tag{9b}$$

$$\psi_\zeta = (\alpha_1^2 + k - 1)\zeta - \frac{(1-\varepsilon_1)(1-\upsilon)\zeta}{\rho_1^3} - \frac{(1-\varepsilon_2)\upsilon\zeta}{\rho_2^3}. \tag{9c}$$

3.1.1 Locations of equilibrium points during in-plane motion (i.e. $\xi \neq 0, \eta \neq 0, \zeta = 0$)

During in-plane motion, we have plotted graphs for the locations of the equilibrium points in four cases. In the classical case, we found well known five equilibrium points in which three are collinear and other two are triangular equilibrium points (Fig. 2a). In the variable mass case, we found five equilibrium points but the locations of the equilibrium points are different from the classical case (Fig. 2b). In the solar radiation case, we found seven equilibrium points which have different locations from the classical case (Fig. 2c). On the other hand with the Albedo effects, we found seven equilibrium points which are similar to the case of solar radiation pressure but different from the other two cases (Fig. 2d). In all the figures black stars denote the locations of the primaries.

3.1.2 Locations of equilibrium points during out of plane (i.e. $\xi \neq 0, \eta = 0, \zeta \neq 0$ and $\xi = 0, \eta \neq 0, \zeta \neq 0$)

During out of plane (i.e. $\xi \neq 0, \eta = 0, \zeta \neq 0$), we found three equilibrium points in all four cases (Fig. 3). In the classical case, L_1 is left side of the primary m_2, L_2 is in between both the primaries and L_3 is right side of the primary m_1. But in the other three cases, L_1 is in between both the primaries, L_2 is left side of the primary m_2 and L_3 is right side of the primary m_1. The black stars denote the locations of the primaries m_1 and m_2.

On the other hand, during the out of plane (i.e. $\xi = 0, \eta \neq 0, \zeta \neq 0$), we found three equilibrium points (Fig. 4). Where the black orbit is for classical case, green orbit is for the variable mass case, magenta orbit is for the solar radiation case and cyan orbit is for Albedo effect. Magenta orbit is not visible because this and cyan orbits are overlapped on each other.

3.2 Periodic orbits

We have drawn the periodic orbits in four cases. In the classical case, we found that the orbit is periodic (in black color) but in the other three cases orbits are not periodic (Fig. 5).

3.3 Poincaré surface of section

We also have drawn the Poincaré surface of sections for the four cases in both the $(\xi - \xi')-$plane (Fig. 6) and the $(\eta - \eta')-$plane (Fig.7-a,b). We found that in the $(\xi - \xi')-$plane, the surfaces are shrinking for the cases from classical case to Albedo effect and in the $(\eta - \eta')-$plane, the surface has dumbbell shape in classical case and in the other three cases surfaces have petal shapes which are also shrinking.

3.4 Basins of attraction

In this section, we have drawn the basins of attraction for the circular restricted three body problem by using Newton-Raphson iterative method for the four cases. The iterative algorithm of our problem is given by the system

$$\begin{cases} \xi_{n+1} = \xi_n - \left(\dfrac{\psi_\xi \psi_{\eta\eta} - \psi_\eta \psi_{\xi\eta}}{\psi_{\xi\xi}\psi_{\eta\eta} - \psi_{\xi\eta}\psi_{\eta\xi}} \right)_{(\xi_n, \eta_n)}, \\ \eta_{n+1} = \eta_n - \left(\dfrac{\psi_\eta \psi_{\xi\xi} - \psi_\xi \psi_{\eta\xi}}{\psi_{\xi\xi}\psi_{\eta\eta} - \psi_{\xi\eta}\psi_{\eta\xi}} \right)_{(\xi_n, \eta_n)}. \end{cases} \tag{9}$$

Where ξ_n, η_n are the values of $\xi$and ηcoordinates of the n^{th} step of the Newton-Raphson iterative process. The initial point (ξ, η) is a member of the basin of attraction of the root if this point converges rapidly to one of the equilibrium points. This process stops when the successive approximation converges to an attractor.For the classification of the equilibrium points on the $(\xi, \eta)-$plane, we

used color code. For the classical case (Fig. 8), L_1, L_2 and L_3 represent cyan color region, L_4 represents blue color region and L_5 represents green color region. The basin of attraction corresponding to the equilibrium points L_1, L_2, L_3, L_4 and L_5 extend to infinity. For the variable mass case (Fig. 9), L_1 and L_3 represent red color regions, L_2 represents cyan color region, L_4 represents pink color region and L_5 represents yellow color region. The basin of attraction corresponding to the equilibrium points L_1, L_3, L_4 and L_5 extend to infinity but corresponding to the equilibrium point L_2, it covers finite area. On the other hand, for the solar radiation pressure and Albedo effect (Fig. 10, Fig. 11), L_1 and L_3 represent red color regions, L_2, L_6 and L_7 represent blue color regions, L_4 represents pink color region and L_5 represents light green color region. The basins of attraction corresponding to the equilibrium points L_1, L_3, L_4 and L_5 extend to infinity but the equilibrium points L_2, L_6 and L_7 cover finite area. In this way a complete view of the basin structures created by the attractors. We can observe in detail from the zoomed part of all the figures in Fig. 8(b), Fig. 9(b), Fig. 10(b), Fig. 11(b). The black points and black stars denote the location of the equilibrium points and the location of the primaries respectively. We also observed that the basins of attraction are shrinking from the classical case to Albedo effect.

3.5 Surfaces

We have drawn the surfaces of the motion of the infinitesimal body under the effect of Albedo in two cases: i- The surfaces with the variation of mass parameter (Fig. 12 (a)). ii. The surfaces with the variation of Albedo (Fig. 12 (b)), by considering equations 9*a* and 9*b*. And observed that there are no significant difference in these two surfaces.

4. Stability of the equilibrium points under the effect of Albedo

We can examine the stability of the equilibrium points under the effect of Albedo by taking $\xi = \xi_0 + \alpha,\ \eta = \eta_0 + \beta,\ \zeta = \zeta_0 + \gamma$ in system (6), we get

$$\begin{cases} \alpha'' - 2\,\beta' - \alpha_1\alpha' = \alpha\ \psi^0_{\xi\xi} + \beta\ \psi^0_{\xi\eta} + \gamma\ \psi^0_{\xi\zeta} \\ \beta'' + 2\,\alpha' - \alpha_1\beta' = \alpha\ \psi^0_{\eta\xi} + \beta\ \psi^0_{\eta\eta} + \gamma\ \psi^0_{\eta\zeta} \\ \gamma'' - \alpha_1\gamma' = \alpha\ \psi^0_{\zeta\xi} + \beta\ \psi^0_{\zeta\eta} + \gamma\ \psi^0_{\zeta\zeta}. \end{cases} \tag{10}$$

Where $\alpha,\ \beta$ and γ are the small displacements of the infinitesimal body from the equilibrium point. The superscript zero denotes the value at the equilibrium point.

To solve system (10), let $\alpha = Ae^{\lambda\tau},\ \beta = Be^{\lambda\tau},\ \gamma = Ce^{\lambda\tau}$, where A, B and C are parameters. Substituting these values in system (10) and rearranging, we get:

$$(11)\qquad \begin{cases} A(\lambda^2-\alpha_1\lambda-\psi^0_{\xi\xi})-B(2\lambda+\psi^0_{\xi\eta})-C\psi^0_{\xi\zeta}=0,\\ A(2\lambda-\psi^0_{\eta\xi})+B(\lambda^2-\alpha_1\lambda-\psi^0_{\eta\eta})-C\psi^0_{\eta\zeta}=0,\\ -A\psi^0_{\zeta\xi}-B\psi^0_{\zeta\eta}+C(\lambda^2-\alpha_1\lambda-\psi^0_{\zeta\zeta})=0. \end{cases}$$

The system (11), will have a non-trivial solution for A, B and C if

$$\begin{vmatrix} \lambda^2-\alpha_1\lambda-\psi^0_{\xi\xi} & -(2\lambda+\psi^0_{\xi\eta}) & -\psi^0_{\xi\zeta}\\ 2\,\lambda-\psi^0_{\eta\xi} & \lambda^2-\alpha_1\lambda-\psi^0_{\eta\eta} & -\psi^0_{\eta\zeta}\\ -\psi^0_{\zeta\xi} & -\psi^0_{\zeta\eta} & \lambda^2-\alpha_1\lambda-\psi^0_{\zeta\zeta} \end{vmatrix}=0,$$

which is equivalent to

$$\begin{aligned} &\lambda^6-3\alpha_1\lambda^5+\lambda^4(4+3\alpha_1^2-\psi^0_{\xi\xi}-\psi^0_{\eta\eta}-\psi^0_{\zeta\zeta})\\ &+\alpha_1\lambda^3(-4-\alpha_1^2+2\,\psi^0_{\xi\xi}+2\,\psi^0_{\eta\eta}+2\,\psi^0_{\zeta\zeta})\\ &+\lambda^2(-\psi_{\xi\eta})^0)^2-(\psi^0_{\xi\zeta})^2+\psi^0_{\xi\xi}\,\psi^0_{\eta\eta}-(\psi^0_{\eta\zeta})^2-4\psi^0_{\zeta\zeta}+\psi^0_{\xi\xi}\psi^0_{\zeta\zeta}+\psi^0_{\zeta\zeta}\,\psi^0_{\eta\eta}\\ &-\alpha_1^2\,\psi^0_{\xi\xi}-\alpha_1^2\,\psi^0_{\eta\eta}-\alpha_1^2\,\psi^0_{\zeta\zeta})\\ &+\alpha_1\lambda((\psi^0_{\xi\eta})^2+(\psi^0_{\xi\zeta})^2-\psi^0_{\xi\xi}\,\psi^0_{\eta\eta}+(\psi^0_{\eta\zeta})^2-\psi^0_{\xi\xi}\,\psi^0_{\zeta\zeta}-\psi^0_{\eta\eta}\,\psi^0_{\zeta\zeta})\\ &+((\psi^0_{\xi\zeta})^2\,\psi^0_{\eta\eta}-2\,\psi^0_{\xi\eta}\,\psi^0_{\xi\zeta}\,\psi^0_{\eta\zeta}+\psi^0_{\xi\xi}\,(\psi^0_{\eta\zeta})^2\\ &+(\psi^0_{\xi\eta})^2\,\psi^0_{\zeta\zeta}-\psi^0_{\xi\xi}\,\psi^0_{\eta\eta}\,\psi^0_{\zeta\zeta})=0. \end{aligned}\qquad (12)$$

We have solved the equation (12) for each value of the equilibrium point and found that in all the cases, λ has complex values and at least one of them has positive real value. Hence all the equilibrium points are unstable.

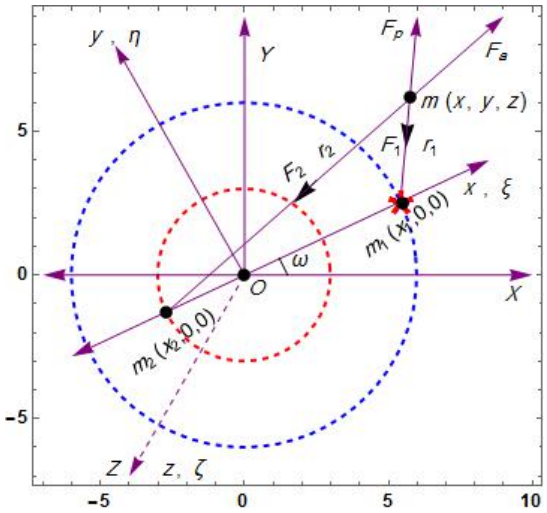

Figure 1: The geometry of the problem with Albedo

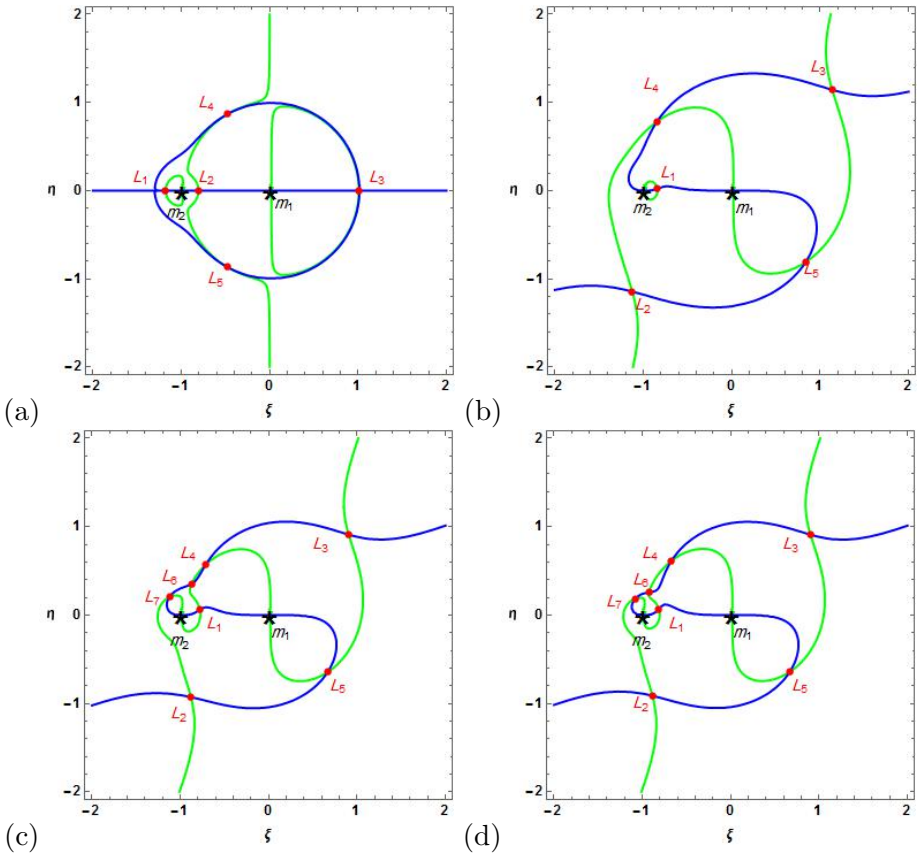

Figure 2: The locations of equilibrium points during in-plane motion (i.e. $\xi \neq 0, \eta \neq 0, \zeta = 0$) in four cases: a. Classical case, b. Variation of masses, c. Solar radiation pressure, d. Albedo effect.

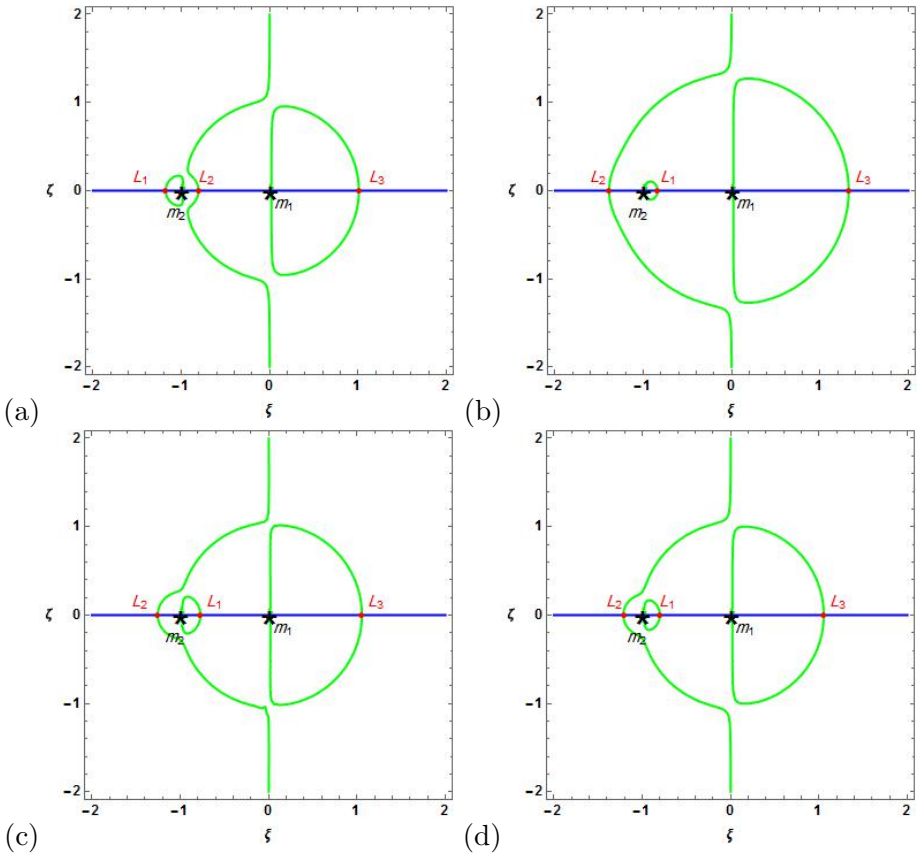

Figure 3: The locations of equilibrium points during out of plane motion (i.e. $\xi \neq 0, \eta = 0, \zeta \neq 0$) in four cases: a. Classical case, b. Variation of masses, c. Solar radiation pressure, d. Albedo effect.

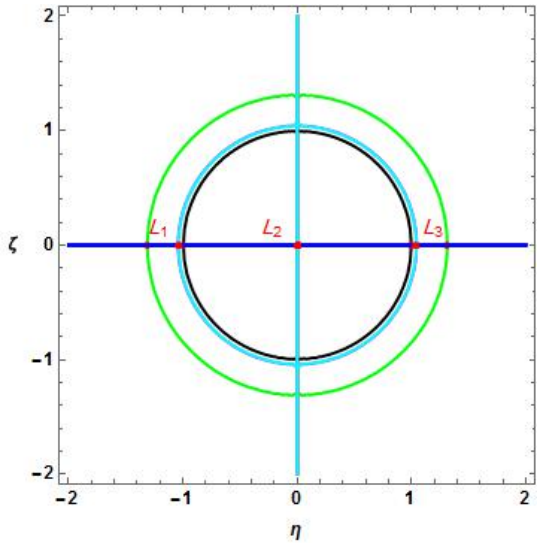

Figure 4: The locations of equilibrium points during out of plane motion (i.e.$\xi = 0, \eta \neq 0, \zeta \neq 0$) in four cases: a. Classical case (Black orbit), b. Variation of masses (Green orbit), c. Solar radiation pressure (Magenta orbit), d. Albedo effect (Cyan orbit). Magenta orbit is covered by Cyan orbit.

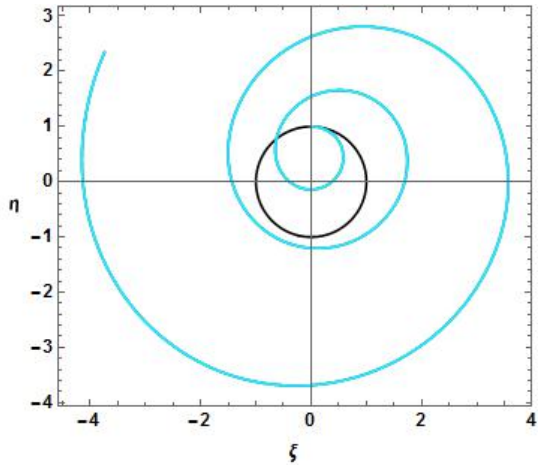

Figure 5: Periodic Orbits in four cases: a- Black, b- Green, c- Magenta, d- Cyan. But Green, Magenta and cyan are overlapped.

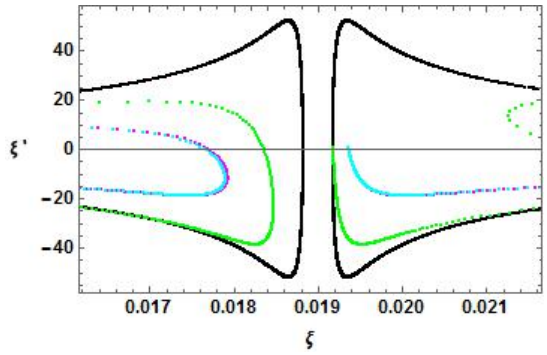

Figure 6: Poincaré surface of sections for four cases: Classical case (Black curve), variable mass case (Green curve), solar radiation pressure (Magenta curve), Albedo effect (Cyan curve).

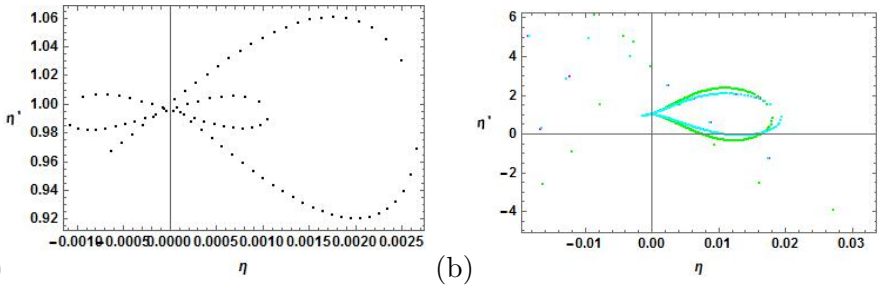

(a) (b)

Figure 7: Poincaré surface of sections for four cases: (a) Classical case (Black curve),(b) (variable mass case (Green curve), solar radiation pressure (Magenta curve), Albedo effect (Cyan curve)).

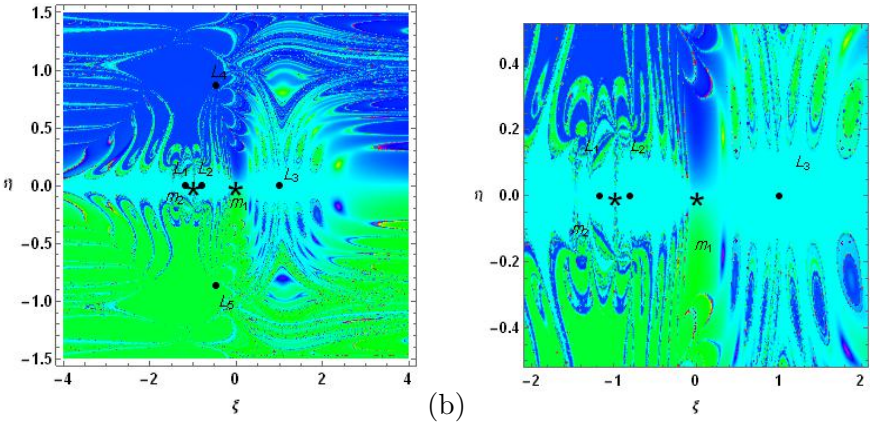

(a) (b)

Figure 8: (a): The basin of attraction for the classical case. (b): Zoomed image of (a) near the primaries

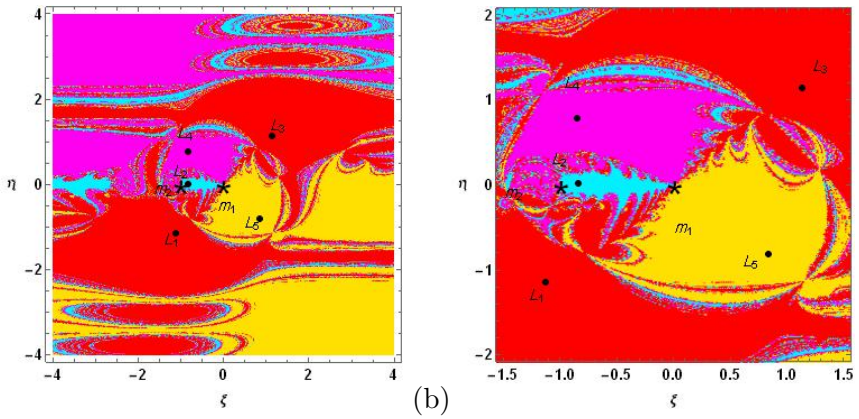

Figure 9: (a): The basin of attraction for the variable mass case. (b): Zoomed image of (a) near the primaries.

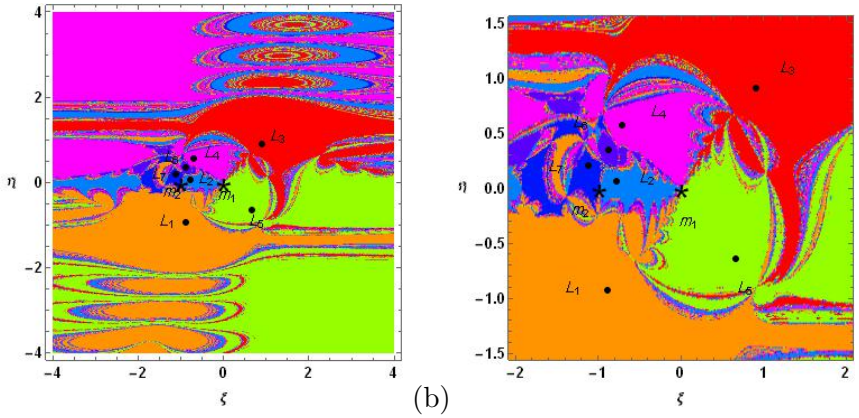

Figure 10: (a): The basin of attraction for the solar radiation pressure case. (b): Zoomed image of (a) near the primaries.

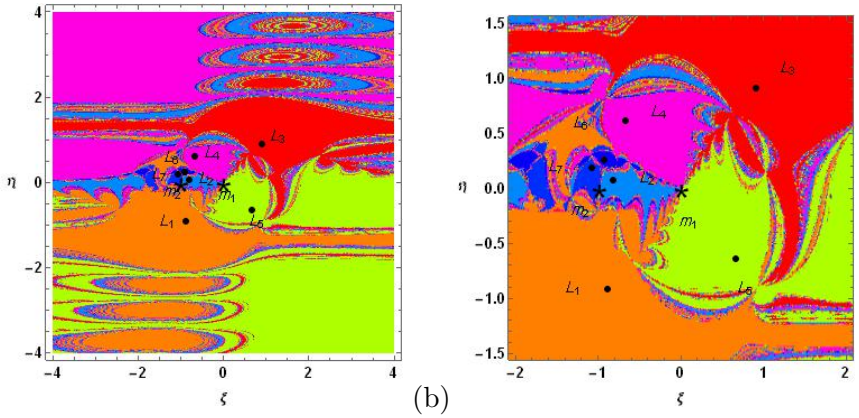

Figure 11: (a): The basin of attraction for the Albedo case. (b): Zoomed image of (a) near the primaries.

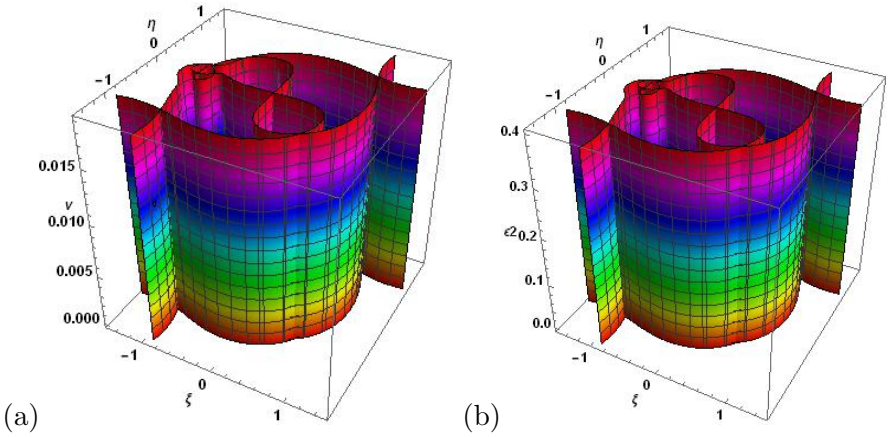

Figure 12: (a) Surfaces with variation of mass parameter. (b): Surfaces with variation of Albedo

5. Conclusion

We have investigated the effect of Albedo in the circular restricted three body problem with variable masses. The equations of motions when the masses of the primaries as well as the infinitesimal body varies, have been evaluated, which are different from the classical case by the variation parameters α_1 and k and the radiations effect ε_1 and ε_2 and also the expression for the variation of Jacobi integral constant have been evaluated. Here all the graphical works have been done by the software package Mathematica in four different cases. We have drawn the equilibrium points during in-plane and out of plane motions. During in-plane motion (Fig. 2), we found five equilibrium points in which three are collinear and two are triangular points in the classical case, in the variable mass case we found five equilibrium points, in the solar radiation and albedo case we found seven equilibrium points. During out-of-plane motions (Fig. 3, Fig. 4), we got three equilibrium points in all four cases. The black stars denote the location of the primaries. The periodic orbits have been drawn in these four cases (Fig. 5). In the classical case orbit is periodic but in the other three cases orbits are not periodic. The poincaré surface of sections have been determined in two phase spaces ($\xi - \xi'$ and $\eta - \eta'$). In $(\xi - \xi')-$plane (Fig. 6), the curves are shrinking and in $(\eta - \eta')-$plane (Fig. 7-a, b), we got dumbbell shape in the classical case and in the other three cases, we got petal shapes. In this case the curves are shrinking.

The Newton-Raphson basins of attraction have been studied for four cases (Fig. 8, Fig. 9, Fig. 10, Fig. 11). For the classification of the equilibrium points on the $(\xi - \eta)-$plane, we used color code. These points will be clearly visible in the zoomed part of all the figures near the primaries (ie. Fig. 8 b, Fig. 9 b, Fig. 10 b, Fig. 11 b). It is observed that the basins of attraction are shrinking. We also have drawn the surfaces with the variation of mass parameter (Fig. 12

(a)) and with the variation of Albedo (Fig. 12 (b)) and no significant difference have been found in both surfaces. Finally, we have examined the stability of the equilibrium points in the circular restricted three body problem under the effect of Albedo and found that all the equilibrium points are unstable.

Acknowledgements

We are thankful to the Deanship of Scientific Research and the Department of Mathematics, College of Science in Zulfi, Majmaah University, Kingdom of Saudi Arabia, for providing all the research facilities in the completion of this research work.

References

[1] A. AbdulRaheem, J. Singh, *Combined effects of perturbations, radiation and oblateness on the stability of equilibrium points in the restricted three body problem*, The Astronomical Journal, 131 (2006), 1880-1885.

[2] E.I. Abouelmagd, M.A. Sharaf, *The motion around the libration points in the restricted three-body problem with the effect of radiation and oblateness*, Astrophys. Space sci., 344 (2013), 321-332.

[3] E.I. Abouelmagd, A. Mostafa, *Out of plane equilibrium points locations and the forbidden movement regions in the restricted three-body problem with variable mass*, Astrophys. Space Sci., 357 (2015), 58, DOI 10.1007/s10509-015-2294-7.

[4] A.A. Ansari, *Stability of the equilibrium points in the photogravitational circular restricted four body problem with the effect of perturbations and variable mass*, Science International (Lahore), 28 (2016), 859- 866.

[5] A.A. Ansari, M. Alam, *Dynamics in the circular restricted three body problem with perturbations*, International Journal of Advanced Astronomy, 5(1) (2017), 19-25.

[6] A.A. Ansari, *The circular restricted four body problem with variable masses*, Nonlinear Science Letters A, 8 (3) (2017), 303-312.

[7] L. Anselmo, P. Farinella, A. Milani, A.M. Nobili, *Effects of the earth-reflected sunlight on the orbit of the LAGEOS Satellite*, Astron. Astrophys, 117 (1983), 3-8.

[8] P. Appel, *Attitude estimation from magnetometer and earth-albedo-corrected coarse sun sensor measurments*, Acta Astronautica, 56 (2005), 115-126.

[9] M.C. Asique et al., *On the photogravitational R4BP when the third primary is a triaxial rigid body*, Astrophys. Space Sci., 361 (2016), 379.

[10] S.C. Assis et al., *Escape dynamics and fractal basin boundaries in the planar earth-moon system*, Celest. Mech. Dyn. Astr., 120 (2014), 105-130.

[11] K.B. Bhatnagar, J.M. Chawla, *A study of the lagrangian points in the photogravitational restricted three body problem*, Indian J. pure and applied math., 10(11) (1979), 1443-1451.

[12] K.B. Bhatnagar, U. Gupta, R. Bhardwaj, *Effect of perturbed potential on the non-linear stability libration point L_4 in the restricted problem*, Celest. Mech. Dy. Astro., 59 (1994), 345-374.

[13] A. Chakraborty, A. Narayan, A. Shrivastava, *Existence and stability of collinear points in elliptic restricted three body problem with radiating and oblate primaries*, International Journal of Advanced Astronomy, 4(2) (2016), 95-104.

[14] Y.A. Chernikov, *The photogravitational restricted three body problem*, Soviet Astronomy, 40(1), July-Aug. (1970).

[15] C.N. Douskos, *Collinear equilibrium points of Hill's problem with radiation pressure and oblateness and their fractal basins of attraction*, Astrophys. Space Sci., 326 (2010), 263-271.

[16] S.V. Ershkov, *The Yarkovsky effect in generalized photogravitational three body problem*, Planetary and Space Sci., 73 (2012), 221-223.

[17] M.J. Idrisi, *A study of Libration Points in Modified CR3BP under Albedo Effect when smaller Primary is an Ellipsoid*, J. of Astronaut. Sci, (2017), DOI 10.1007/s40295-017-0115-7.

[18] M.J. Idrisi, *A study of libration points in CR3BP under albedo effect,* International Journal of Advanced Astronomy, 5 (1) (2017), 1-6.

[19] J.H. Jeans, *Astronomy and Cosmogony*, Cambridge University Press, Cambridge, (1928).

[20] R. Kumari, B.S. Kushvah, *Stability regions of equilibrium points in the restricted four body problem with oblateness effects*, Astrophys. Space Sci., 349 (2014), 693-704.

[21] A.L. Kunitsyn, A.T. Tureshboev, *On the collinear libration points in the photogravitational three body problem*, Celest. Mech., 35 (1985), 105-112.

[22] G. Matthies, *An optimal three points eight-order iterative method without memory for solving non-linear equations with its dynamics*, Japan J. Indust. Applied Math, 33 (2016), 751-766.

[23] I.V. Meshcherskii, *Works on the Mechanics of Bodies of Variable Mass*, GITTL, Moscow, (1952).

[24] F. Mignard, *Stability of L_4 and L_5 against radiation pressure*, Celest. Mech., 34 (1984), 275-287.

[25] A. Mittal et. al., *Stability of libration points in the restricted four-body problem with variable mass*, Astrophysics and space science, 361(2016), 329, DOI 10.1007/s10509-016-2901-2.

[26] F.R. Moulton, *An introduction to celestial mechanic*, Second ed. Dover, New York, (1914).

[27] L.J.H. Paricio, *Bivariate Newton-Raphson method and toroidal attraction basins*, Numerical Algo., 71 (2016), 349-381.

[28] A.A. Perezhogin, *Stability of the sixth and seventh libration points in the photogravitational restricted circular three body problem*, Soviet Astronomy letters, 2 (1976), 172.

[29] N. Pushparaj, R.K. Sharma, *Interior resonance periodic orbits in the photogravitational restricted three-body problem*, Advances in astrophysics, 1(2)(2017), 25-34.

[30] E.M. Rocco, *Evaluation of the terestrial Albedo-Applied to some scientific missions*, Space Sci. Rev., 151 (2009), 135-147, DOI 10.1007/s11214-009-9622-6.

[31] D.W. Schuerman, *The restricted three-body problem including radiation pressure*, The Astrophysical Journal, 238 (1980), 337-342.

[32] R.K. Sharma, *Perturbations of Lagrangian points in the restricted three-body problem,* Indian Journal of Pure and Applied Mathematics, 6 (1975), 1099-1102.

[33] R.K. Sharma, *The linear stability of libration points of the photogravitational restricted three body problem when the smaller primary is an oblate spheroid*, Astrophys. Space Sci., 135 (1987), 271-281.

[34] J.F.L. Simmons, A.J.C. McDonald, J.C. Brown, *The restricted three body problem with radiation pressure.* Celest. Mech., 35 (1985), 145-187.

[35] J. Singh, *Effect of perturbations on the location of equilibrium points in the restricted problem of three bodies with variable mass*, Celest. Mech., 32 (1984), 297-305.

[36] J. Singh, B. Ishwar, *Effect of perturbations on the stability of triangular points in the restricted problem of three bodies with variable mass*, Celest. Mech., 35 (1985), 201-207.

[37] J. Singh, *Photogravitational restricted three body problems with variable mass*, Indian Journal of Pure and Applied Math., 32 (2) , (2003), 335-341.

[38] J. Singh, O. Leke, *Stability of photogravitational restricted three body problem with variable mass*, Astrophys. Space Sci., 326 (2) (2010), 305-314.

[39] J. Singh, A.E. Vincent, *Equilibrium points in the restricted four-body problem with radiation pressure*, Few-Body Syst., 57 (2016), 83-91.

[40] P.V. Subbarao, R.K. Sharma, *A note on the stability of the triangular points of equilibrium in the restricted three body problem*, Astron. Astrophys, 43 (1975), 381-383.

[41] M.J. Zhang, C.Y. Zhao, Y.Q. Xiong, *On the triangular libration points in photo-gravitational restricted three body problem with variable mass*, Astrophysics Space Sci., 337 (2012), 107-113, DOI 10.1007/s10509- 011-0821-8.

[42] E.E. Zotos, *Fractal basins of attraction in the planar circular restricted three body problem with oblateness and radiation pressure* , Astrophys. Space Sci. 181(17) (2016).

[43] E.E. Zotos, *Fractal basins boundaries and escape dynamics in a multi-well potential*, Non-linear Dyn. 85 (2016), 1613- 1633.

[44] E.E. Zotos, *Investigating the Newton-Raphson basins of attraction in the restricted three body problem with modified Newtonian gravity*, J. Appl. Math. Comput., Oct (2016), 1-19.

[45] E.E. Zotos, *Revealing the basins of convergence in the planar equilateral restricted four body problem*, Astrophys. Space Sci., 362(2) (2017).

Accepted: 9.06.2017